Chemistry 5325/5326
Inorganic Chemistry
Spring Semester 2012

Department of Chemistry
http://homepages.uconn.edu/rossi
angelo.rossi@uconn.edu

Predicting the Structures of Rhodium Carbonyl Clusters

The structures of neutral rhodium carbonyl clusters containing two, four, and six rhodium atoms have been known for some time.

The paper by Ingmar Swart, Frank M. F. de Groot, Bert M. Weckhuysen, David M. Rayner, Gerard Meijer, and André Fielicke *The Effect of Charge on CO Binding in Rhodium Carbonyls: From Bridging to Terminal CO*, J. Am. Chem. Soc. **2008**, *130*, 2126-2127 investigates the structures of the monocation rhodium carbonyl clusters via infrared multiphoton dissociation spectroscopy (IR-MPD), comparing experimental results to those predicted from computational modeling.

These are ideal problems to apply simple the tools of group theory to predict distinguishing features in the IR spectrum of each possible structure.

For this part of the project we will focus primarily on the υ_{CO} stretching frequencies. The stretching frequencies of terminally bound CO ligands (2060-2100 cm^{-1}) are typically well separated from those of bridging CO ligands (1750-1900 cm^{-1}), and so these vibrations could form separate basis sets for symmetry analysis.

Although static images from the paper are given below, PDB files each of these structures are also available for visualization with applications such as Jmol and VMD by clicking on the link next to the appropriate structure.

Goals of this project include the use of the tools of group theory and symmetry:

1. to predict how many υ_{CO} stretching frequencies one would see in the IR spectrum of each possible structure, and

2. to write a representation for the υ_{CO} stretching frequencies in each structure and determine how many peaks one would expect to see in the terminal and bridging CO regions of the IR spectrum.

The idea is to predict the structure of $[Rh_n(CO)_m]^+$ complexes based both on the experimental structures of neutral species and calculations performed on both neutral and analagous charged complexes.

Department of Chemistry
http://homepages.uconn.edu/rossi
angelo.rossi@uconn.edu

Calculated structures of $Rh_2(CO)_8$: the bridged structure is slightly lower in energy than the all-terminal structure, in agreement with experiment.

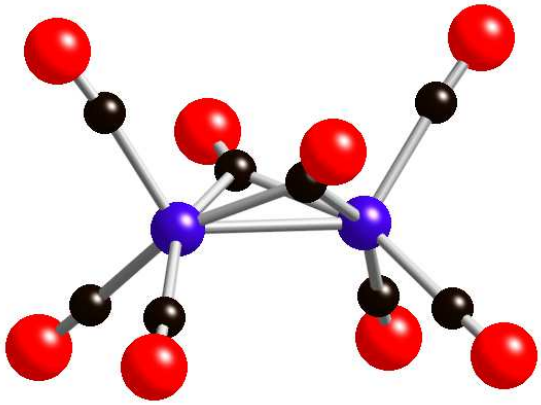

All Bridging COs

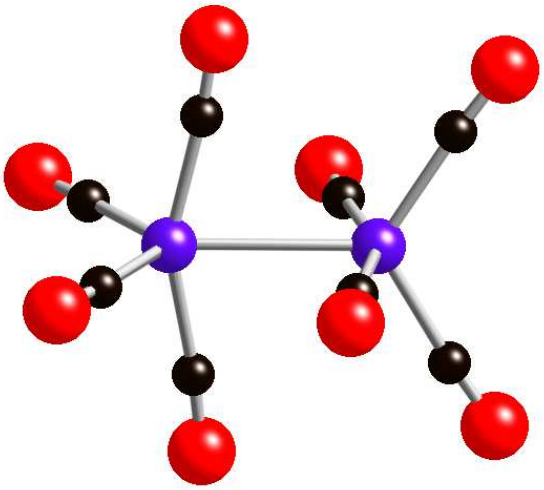

All Terminal COs

Calculated structures for $[Rh_2(CO)_8]^+$

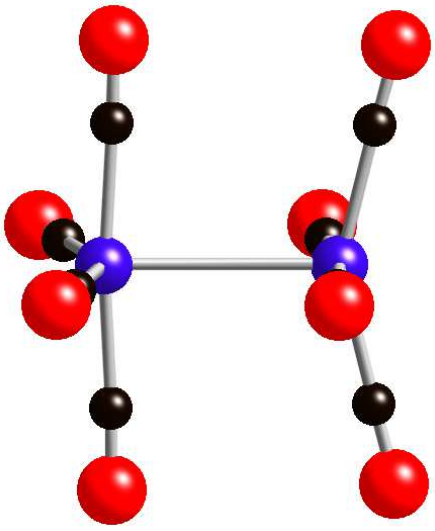

Lowest Energy Structure

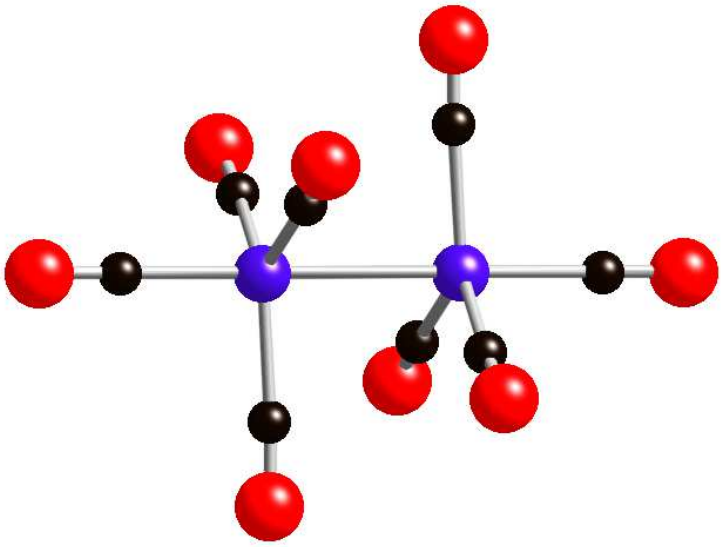

Another Possible Structure for $[Rh_2(CO)_8]^+$

Department of Chemistry
http://homepages.uconn.edu/rossi
angelo.rossi@uconn.edu

Calculated Structures for $[Rh_3(CO)_9]^+$

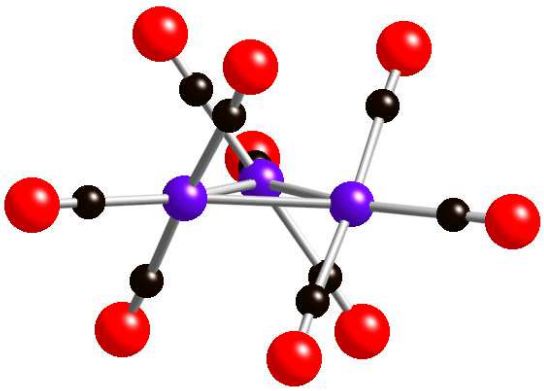

Lowest Energy Structure

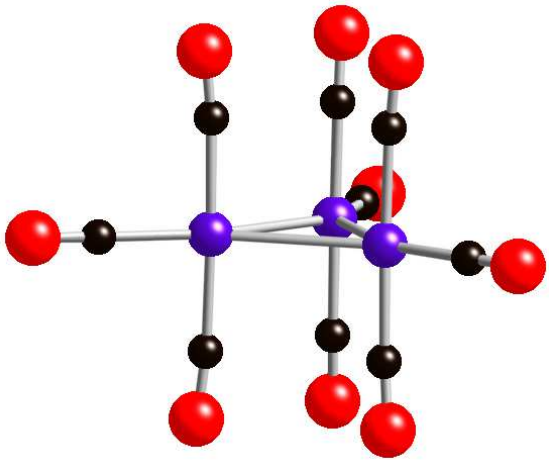

Another Possible Structure for $[Rh_3(CO)_9]^+$

Calculated structures of $Rh_4(CO)_{12}$, $[Rh_4(CO)_{12}]^+$: the neutral structure agrees with experiment.

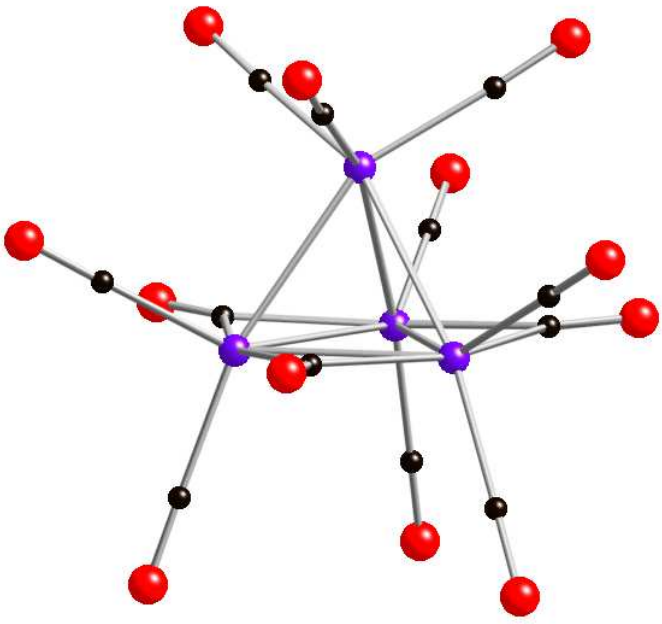

Known Structure of Neutal Cluster

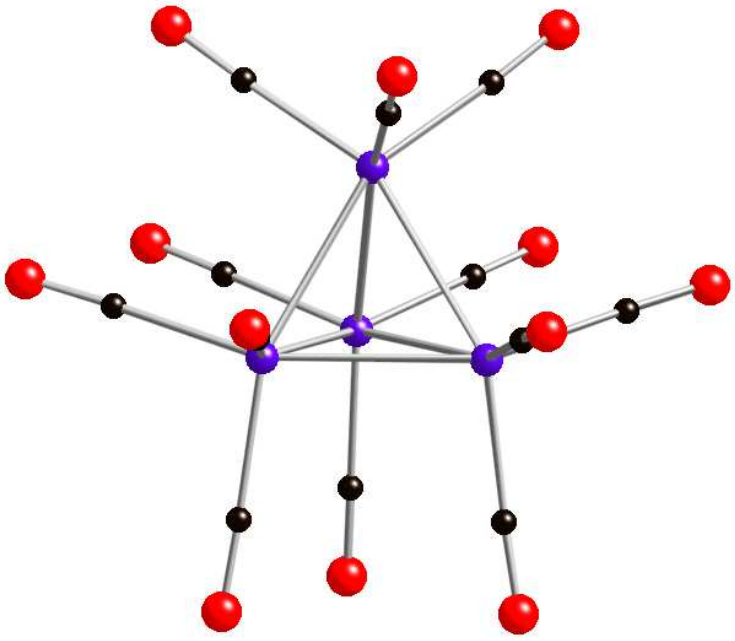

Proposed Monocationic Structure

J|A|C|S
COMMUNICATIONS

Published on Web 01/29/2008

The Effect of Charge on CO Binding in Rhodium Carbonyls: From Bridging to Terminal CO

Ingmar Swart, Frank M. F. de Groot,* Bert M. Weckhuysen, David M. Rayner,* Gerard Meijer, and André Fielicke*

Inorganic Chemistry and Catalysis, Faculty of Science, Utrecht University, Sorbonnelaan 16, 3584 CA, Utrecht, The Netherlands, Steacie Institute for Molecular Sciences, National Research Council, 100 Sussex Drive Ottawa, Ontario, K1A 0R6, Canada, and Fritz-Haber-Institut der Max-Planck-Gesellschaft, Faradayweg 4-6, 14195 Berlin, Germany

Received September 20, 2007; E-mail: f.m.f.degroot@uu.nl; david.rayner@nrc-cnrc.gc.ca; fielicke@fhi-berlin.mpg.de

Changing the electron density of a catalyst can have a profound influence on its selectivity and activity. For this reason, electronic promoter materials are often added to a catalyst to tailor the electron density of the active particle and to obtain optimal performance.[1] Despite the widespread use of electronic promoters, the mechanisms responsible for the observed effect(s) are often poorly understood. For CO oxidation over a Pt catalyst, the activity increases with electron density.[2] In contrast, the hydrogenation of CO over cobalt- and rhodium-based catalysts is found to be more active and more selective upon reducing the electron density of the metal particles.[3,4] This change in electron density also leads to a decrease in the ratio of bridge to linear-bound CO but the mechanism behind this destabilization of bridge-bound CO is unknown.[3,5]

We address the issue of charge-induced changes in the binding of CO to metal centers by focusing on rhodium carbonyls as models. Rhodium-based catalysts have been used for many reactions involving CO.[6] The structures of the neutral saturated carbonyl complexes containing two, four, and six Rh atoms are well-known,[7−10] but little is known about the charged complexes. We establish the structures of the cations by infrared multiple photon dissociation (IR-MPD) spectroscopy. By comparing the structures of the cationic species with structures of the corresponding neutral complexes, information regarding the effect of charge on the binding geometry of CO is obtained.

The experimental procedures for IR-MPD spectroscopy have been described in detail elsewhere.[11−13] Briefly, a molecular beam of cluster complexes, generated in a laser ablation source coupled with a reaction channel, is overlapped with a counter-propagating beam of IR photons delivered by the Free Electron Laser for Infrared eXperiments (FELIX).[14] When the laser frequency is resonant with an IR-active vibration of a complex, it can absorb several photons and subsequently undergo fragmentation. The vibrational spectra are obtained by monitoring the changes in the cluster mass distribution as a function of IR frequency. The experimental spectra are complemented with density functional theory (DFT) calculations (B3LYP/TZVP, see Supporting Information) to obtain information on cluster geometries and electronic structure.[15]

Upon introduction of CO in the reactor channel, the Rh_n^+ clusters bind multiple CO molecules. The pressure in the reactor channel was increased until the resulting molecular beam distribution did not change anymore, that is, when the clusters were saturated with carbon monoxide.[16] The complexes saturate as $Rh(CO)_5^+$, $Rh_2(CO)_8^+$, $Rh_3(CO)_9^+$, $Rh_4(CO)_{12}^+$, $Rh_5(CO)_{14}^+$, and $Rh_6(CO)_{16}^+$. The saturation numbers of the cationic rhodium dimer, tetramer, and hexamer are the same as those of the corresponding neutral clusters. Binary tri- and pentanuclear rhodium cluster carbonyls have not been identified before.

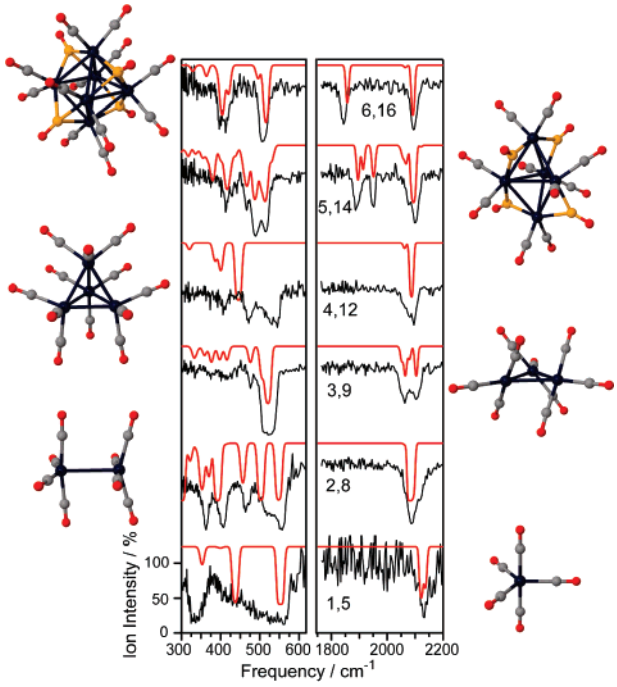

Figure 1. Experimental (black) and calculated (red) vibrational spectra of $Rh_n(CO)_m^+$ complexes. The values *n*, *m* indicate the number of Rh atoms and CO molecules, respectively. The simulated depletion spectra are based on the calculated single photon absorption spectra. In the complex geometries shown next to the graph, C atoms of μ_1 CO are depicted in gray and C atoms of μ_2 and μ_3 CO are shown in yellow.

The vibrational spectra in the C−O stretching region and the Rh−C stretch and deformation region for complexes with 1−6 metal atoms are shown in Figure 1. Terminally bound CO ligands are present for all complexes (absorption bands between 2060−2100 cm^{-1}) but bridging (μ_2-CO) and/or face capping (μ_3-CO) carbonyls (absorption bands between 1750 and 1900 cm^{-1}) are only present for $Rh_5(CO)_{14}^+$ and $Rh_6(CO)_{16}^+$. The cationic carbonyl complexes with 1−4 metal atoms therefore contain only terminally bound CO ligands.[17] The DFT calculations confirm this assignment and also predict that vibrational modes associated with bridge bound CO in isomers of complexes with 2−4 metal atoms have significant IR intensities which should be observed experimentally. The cluster structures and the calculated spectra are shown together with the IR-MPD spectra in Figure 1. The calculated and experimental spectra are in good agreement in both the C−O stretching range, ν(CO), as well as in the Rh−C stretch and deformation region,

10.1021/ja0772795 CCC: $40.75

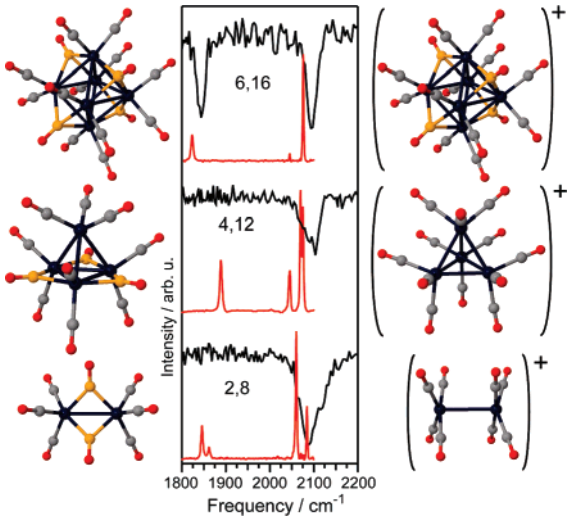

Figure 2. Experimental vibrational spectra of $Rh_2(CO)_8^{+/0}$, $Rh_4(CO)_{12}^{+/0}$, and $Rh_6(CO)_{16}^{+/0}$ (cations, black; neutrals, red; bottom to top) in the ν(CO) range. Structures for the neutral complexes are shown on the left and for the cations on the right. In the complex geometries shown next to the graph, C atoms of μ_1 CO are depicted in gray and C atoms of μ_2 and μ_3 CO are shown in yellow.

ν/δ(RhC). Only in the case of $Rh_4(CO)_{12}^+$ we find a discrepancy, a band at ~530 cm^{-1} is missing in the simulated spectrum. A possible explanation for this discrepancy is that the complex is distorted from the high-symmetry structure (T_d) shown in Figure 1 or the presence of a second isomer. The lowest energy isomers identified by the calculations are also the ones whose vibrational spectra are in best agreement with the experimental data.

In Figure 2 we compare the vibrational spectra of the neutral (taken from ref 10) and cationic species. It is immediately clear that cationic and neutral $Rh_2(CO)_8$ and $Rh_4(CO)_{12}$ have different structures. The neutral complexes have two and three bridge-bound carbonyl ligands, respectively,[7,10] whereas all CO molecules are terminally bound in $Rh_2(CO)_8^+$ and $Rh_4(CO)_{12}^+$. Removing an electron from the neutral complexes thus leads to a destabilization of the bridge bound carbonyl ligands. In contrast, $Rh_6(CO)_{16}$ does not undergo a structural rearrangement. The metal cores of the cations retain the structure of the neutral compounds.

DFT calculations were performed for neutral complexes as well as for cations in the structure of the neutral clusters to compare the electronic structures. The calculations identify the correct ground state isomers of the neutral complexes. For $Rh_2(CO)_8$, the neutral complex with only terminally bound CO molecules is just 0.09 eV higher in energy. The calculations show that the highest occupied molecular orbital (HOMO) of the complex with the bridging carbonyls is doubly occupied and can be thought of as a combination of rhodium d-orbitals with antibonding $2\pi^*$ orbitals of the bridging CO ligands, the classic back-donation of M−CO binding. The HOMO is bonding with respect to the Rh−μ_2-CO bonds. Ionization removes an electron from the HOMO. Mulliken overlap population analysis shows that the electron density in a single Rh−μ_2-CO bond is reduced by 12% upon removing one electron from the neutral cluster. The $Rh_2(CO)_8^+$ complex is unstable in the structure of the neutral. It is a transition state that is +0.65 eV higher in energy than the isomer with only terminally bound CO. Consequently the complex will undergo a charge induced structural rearrangement. According to our calculations, the accompanying reorganization in electronic structure results in a lengthening of the Rh−Rh bond (see Supporting Information). A similar argument holds for $Rh_4(CO)_{12}$. The HOMO is involved in the binding of the three bridge-bonded CO molecules. Upon removing one electron, the electron density between the rhodium atoms and the bridging CO ligands is reduced by 38%. The destabilization of the bridge-bonded CO molecules leads to a complex with only terminally bound CO. As shown by the experimental and calculated vibrational spectra, the high symmetry (T_d) complex $Rh_6(CO)_{16}$ does not undergo structural rearrangement upon removal of an electron. The HOMO of $Rh_6(CO)_{16}$ is involved in the binding of the face-capping CO. It has t_2 symmetry and is fully occupied, that is, there are six electrons in three equivalent orbitals. This results in a very stable complex. Removing one electron from the HOMO reduces the electron density between the rhodium atoms and the face-capping carbonyl ligands by only 4%, and hence the complex does not undergo reorganization.

In conclusion, a complete series of saturated cationic rhodium carbonyl complexes $Rh_n(CO)_m^+$ ($n = 1-6$) has been structurally characterized. It is shown that the removal of an electron from a metal carbonyl cluster can selectively destabilize bridge-bonded CO molecules. These results provide a possible explanation for effects of promoter materials that are observed for CO bonding on transition-metal catalysts,[2,3] providing information that contributes to understanding the origin of electronic promoter effects in catalysis in general.

Acknowledgment. We gratefully acknowledge the support of the Stichting voor Fundamenteel Onderzoek der Materie (FOM) in providing beam time on FELIX. The authors thank the FELIX staff for their skillful assistance, in particular Dr. B. Redlich and Dr. A.F.G. van der Meer. I.S., F.M.F.d.G., and B.M.W. acknowledge NWO and NRSCC for financial support. Computational time was provided by the SARA supercomputer center in Amsterdam, The Netherlands.

Supporting Information Available: Description of the computational procedure and detailed results. This material is available free of charge via the Internet at http://pubs.acs.org.

References

(1) Ertl, G., Knözinger, H., Weitkamp, J., Eds. *Handbook of Heterogeneous Catalysis;* Wiley-VCH: Weinheim, Germany, 1997; p 2801.
(2) Visser, T.; Nijhuis, T. A.; van der Eerden, A. M. J.; Jenken, K.; Ji, Y.; Bras, W.; Nikitenko, S.; Ikeda, Y.; Lepage, M.; Weckhuysen, B. M. *J. Phys. Chem. B* **2005**, *109*, 3822.
(3) Morales, F.; de Smit, E.; de Groot, F. M. F.; Visser, T.; Weckhuysen, B. M. *J. Catal.* **2007**, *246*, 91.
(4) Koerts, T.; van Santen, R. A. *J. Catal.* **1992**, *134*, 13.
(5) Beutel, T.; Alekseev, O. S.; Ryndin, Y. A.; Likholobov, V. A.; Knozinger, H. *J. Catal.* **1997**, *169*, 132.
(6) Dyson, P. J.; McIndoe, J. S. *Transition Metal Carbonyl Cluster Chemistry;* Gordon and Breach Science Publishers: Amsterdam, The Netherlands, 2000.
(7) Wei, C. H. *Inorg. Chem.* **1969**, *8*, 2384.
(8) Corey, E. R.; Dahl, L. F.; Beck, W. *J. Am. Chem. Soc.* **1963**, *85*, 1202.
(9) Heaton, B. T.; Jacob, C.; Podkorytov, I. S.; Tunik, S. P. *Inorg. Chim. Acta* **2006**, *359*, 3557.
(10) Allian, A. D.; Wang, Y. Z.; Saeys, M.; Kuramshina, G. M.; Garland, M. *Vib. Spectrosc.* **2006**, *41*, 101.
(11) Fielicke, A.; von Helden, G.; Meijer, G.; Pedersen, D. B.; Simard, B.; Rayner, D. M. *J. Phys. Chem. B* **2004**, *108*, 14591.
(12) Swart, I.; Fielicke, A.; Redlich, B.; Meijer, G.; Weckhuysen, B. M.; de Groot, F. M. F. *J. Am. Chem. Soc.* **2007**, *129*, 2516
(13) Oomens, J.; Tielens, A.; Sartakov, B. G.; von Helden, G.; Meijer, G. *Astrophys. J.* **2003**, *591*, 968.
(14) Oepts, D.; van der Meer, A. F. G.; van Amersfoort, P. W. *Infrared Phys. Technol.* **1995**, *36*, 297.
(15) Ahlrichs, R.; Bär, M.; Häser, M.; Horn, H.; Kölmel, C. *Chem. Phys. Lett.* **1989**, *162*, 165.
(16) Fayet, P.; McGlinchey, M. J.; Wöste, L. H. *J. Am. Chem. Soc.* **1987**, *109*, 1733.
(17) The spectra exhibit saturation and broadening of the μ_1 band(s) when repeated at 20 times the IR fluence but no new absorptions. This confirms that noise does not mask low strength transitions. Saturation of the depletion via the μ_1 band(s) confirms that other isomers are not present in significant quantities.

JA0772795

Inorg. Chem. **2009**, *48*, 1599−1605

New Findings in the Chemistry of Iron Carbonyls: The Previously Unreported $[H_{4-n}Fe_4(CO)_{12}]^{n-}$ ($n = 1, 2$) Series of Clusters, Which Fills the Gap with Ruthenium and Osmium

Cristina Femoni, Maria Carmela Iapalucci, Giuliano Longoni, Stefano Zacchini,* and Salvatore Zarra

Dipartimento di Chimica Fisica e Inorganica, Università di Bologna, Viale Risorgimento 4, 40136 Bologna, Italy

Received October 21, 2008

The new $[HFe_4(CO)_{12}]^{3-}$ cluster anion has been obtained in high yields by reduction of $[Fe_4(CO)_{13}]^{2-}$ or $[HFe_3(CO)_{11}]^-$ with a 6 M methylalcoholic KOH solution under a nitrogen atmosphere and isolated with miscellaneous tetrasubstituted ammonium salts. The $[NEt_4]_3[HFe_4(CO)_{12}]$ salt has been characterized by IR, ^1H and ^{13}C NMR, electrospray ionization mass spectrometry, and X-ray studies. Investigation of its protonation reaction afforded spectroscopic proof for the existence of its unstable isomeric $[HFe_4(CO)_{11}(CO\text{-}H)]^{2-}$ and $[H_2Fe_4(CO)_{12}]^{2-}$ conjugated acids. The latter is probably isostructural with the $[H_2Ru_4(CO)_{12}]^{2-}$ congener. The nature of the first protonation product as a $[HFe_4(CO)_{11}(CO\text{-}H)]^{2-}$ adduct, involving an oxygen-bound proton, has been corroborated by the preparation and spectroscopic characterization of the corresponding $[HFe_4(CO)_{11}(CO\text{-}Me)]^{2-}$ dianion. The above findings demonstrate that protonation of a CO-shielded polynuclear metal anion initially occurs on one oxygen atom and then the oxygen-bound proton migrates to the metal cage. Finally, $[HFe_4(CO)_{12}]^{3-}$ and its $[H_2Fe_4(CO)_{12}]^{2-}$ conjugate acid fill the previously existing gap between the chemistry of iron carbonyls and ruthenium and osmium congeners.

Introduction

The chemistry of carbonylferrates and hydridocarbonylferrates is a topic described in most inorganic chemistry textbooks because of its historical, fundamental, and practical importance.[1] Nowadays, the species structurally characterized comprise dianionic carbonylferrates, i.e., $[Fe(CO)_4]^{2-}$,[2] $[Fe_2(CO)_8]^{2-}$,[3] $[Fe_3(CO)_{11}]^{2-}$,[4] and $[Fe_4(CO)_{13}]^{2-}$,[5] as well as the related monohydridocarbonylferrates, $[HFe(CO)_4]^-$,[6] $[HFe_2(CO)_8]^-$,[7] $[HFe_3(CO)_{11}]^-$,[8] and $[HFe_4(CO)_{13}]^-$.[9] Moreover, some paramagnetic carbonylferrates, such as $[Fe_2(CO)_8]^{\bullet-}$, $[Fe_3(CO)_{12}]^{\bullet-}$, and $[Fe_3(CO)_{11}]^{\bullet-}$, have been characterized mainly by electron paramagnetic resonance studies on isotopically enriched (^{13}C, ^{57}Fe) samples.[10,11] The existence of neutral dihydride species, such as $H_2Fe_3(CO)_{11}$ and $H_2Fe_4(CO)_{13}$, was controversial, and their real nature as $HFe_3(CO)_{10}(CO\text{-}H)$ and $HFe_4(CO)_{12}(CO\text{-}H)$ species has been proven in the last 2 decades by multinuclear NMR studies at variable temperature.[12,13]

* To whom correspondence should be addressed. E-mail: zac@ms.fci.unibo.it. Telephone: +39 051 209 3711. Fax: +39 051 2093690.

(1) (a) Brunet, J.-J. *Chem. Rev.* **1990**, *90*, 1041, and reference cited therein. (b) Farmery, K.; Kilner, M.; Greatrex, R.; Greenwood, N. N. *J. Chem. Soc. A* **1969**, 2339.
(2) (a) Chin, H. B.; Bau, R. *J. Am. Chem. Soc.* **1976**, *98*, 2434. (b) Teller, R. G.; Finke, R. G.; Collman, J. P.; Chin, H. B.; Bau, R. *J. Am. Chem. Soc.* **1977**, *99*, 1104.
(3) (a) Chin, H. B.; Smith, M. B.; Wilson, R. D.; Bau, R. *J. Am. Chem. Soc.* **1974**, *96*, 5285. (b) Bhattacharyya, N. K.; Coffy, T. J.; Quintana, W.; Salupo, T. A.; Bricker, J. C.; Shay, T. B.; Payne, M.; Shore, S. G. *Organometallics* **1990**, *9*, 2368. (c) Deng, H.; Shore, S. G. *Inorg. Chem.* **1992**, *31*, 2289.
(4) Lo, F. Y.-K.; Longoni, G.; Chini, P.; Lower, L. D.; Dahl, L. F. *J. Am. Chem. Soc.* **1980**, *102*, 7691.
(5) (a) Doedens, R. J.; Dahl, L. F. *J. Am. Chem. Soc.* **1966**, *88*, 4847. (b) van Buskirk, G.; Knobler, C. B.; Kaesz, H. D. *Organometallics* **1985**, *4*, 149. (c) Femoni, C.; Iapalucci, M. C.; Longoni, G.; Zacchini, S.; Zazzaroni, E. *Dalton Trans.* **2007**, 2644.
(6) Smith, M. B.; Bau, R. *J. Am. Chem. Soc.* **1973**, *95*, 2388.
(7) Chin, H. B.; Bau, R. *Inorg. Chem.* **1978**, *17*, 2314.
(8) (a) Dahl, L. F.; Blount, J. F. *Inorg. Chem.* **1965**, *4*, 1373. (b) Iiskola, E.; Pakkanen, T. A.; Pakkanen, T. T.; Venalainen, T. *Acta Chem. Scand. A* **1983**, *37*, 125.
(9) Manassero, M.; Sansoni, M.; Longoni, G. *J. Chem. Soc., Chem. Commun.* **1976**, 919.
(10) (a) Krusic, P. J.; Morton, J. R.; Preston, K. F.; Williams, A. J.; Lee, F. L. *Organometallics* **1990**, *9*, 697. (b) Krusic, P. J.; San Filippo, J.; Hutchinson, B.; Hance, R. L.; Daniels, L. M. *J. Am. Chem. Soc.* **1981**, *103*, 2129. (c) Krusic, P. J. *J. Am. Chem. Soc.* **1981**, *103*, 2131.
(11) Ragaini, F.; Song, J.-S.; Ramage, D. L.; Geoffroy, G. L.; Yap, G. A. P.; Rheingold, A. L. *Organometallics* **1995**, *14*, 387.
(12) Hodali, H. A.; Shriver, D. F.; Ammlung, C. A. *J. Am. Chem. Soc.* **1978**, *100*, 5239.

10.1021/ic802015f CCC: $40.75
Published on Web 01/21/2009

Conversely, the heavier ruthenium and osmium congeners display a richer chemistry, mainly because of the stronger M−M interactions and the greater size of the metal atoms. In particular, the existence of a fully characterized $[H_{4-n}M_4(CO)_{12}]^{n-}$ (M = Ru, Os; $n = 0-4$) series of tetranuclear clusters is of great relevance to the present work.[14,15] To the best of our knowledge, the existence of analogous iron species was never reported previously.

We came across the $[H_{4-n}Fe_4(CO)_{12}]^{n-}$ ($n = 1, 2$) series of iron carbonyl anions while investigating the behavior of the alkali salts of $[Fe_3(CO)_{11}]^{2-}$, $[Fe_4(CO)_{13}]^{2-}$, and $[Fe_3(\mu_3\text{-}O)(CO)_9]^{2-}$ as starting materials for the synthesis of bimetallic clusters. As a result, we report here the synthesis and structural and spectroscopic characterization of the stable $[HFe_4(CO)_{12}]^{3-}$ hydridocarbonyl cluster anion and spectroscopic evidence for its conversion upon protonation into the unstable $[HFe_4(CO)_{11}(CO\text{-}H)]^{2-}$ and $[H_2Fe_4(CO)_{12}]^{2-}$ conjugate acids.

Experimental Section

General Procedures. All reactions and sample manipulations were carried out using standard Schlenk techniques under a nitrogen atmosphere and in dried solvents. All of the reagents were commercial products (Aldrich) of the highest purity available and were used as received. The $[Fe(DMF)_6][Fe_4(CO)_{13}]$ and $[HNEt_3][HFe_3(CO)_{11}]$ salts have been prepared according to the literature.[1b] Analysis of iron was performed by atomic absorption on a Pye-Unicam instrument. Analyses of carbon, hydrogen, and nitrogen were obtained with a ThermoQuest FlashEA 1112NC instrument. IR spectra were recorded on a Perkin-Elmer Spectrum-One interferometer in CaF_2 cells. Electrospray ionization mass spectrometry (ESI-MS) spectra were recorded on a Waters Micromass ZQ4000 instrument. All NMR measurements were performed on Varian Inova 600 and Mercury Plus 400 instruments. Structure drawings have been performed with *SCHAKAL99*.[16]

Synthesis of $[NEt_4]_3[HFe_4(CO)_{12}]$. KOH (6.6 g, 118 mmol) was dissolved in MeOH (20 mL) and the solution cooled to room temperature. $[Fe(DMF)_6][Fe_4(CO)_{13}]$ (0.64 g, 0.59 mmol) was added in solid and the solution stirred overnight. The product was then precipitated by the slow addition of a large excess of a solution of $[NEt_4]Br$ in water. The solid was recovered by filtration, washed with water (2 × 40 mL), and dried under reduced pressure. The residue was further washed with toluene (30 mL), THF (30 mL), and acetone (30 mL) and finally extracted in CH_3CN (20 mL). Precipitation by the slow diffusion of hexane (5 mL) and diisopropyl ether (50 mL) gave a dark-brown crystalline precipitate of $[NEt_4]_3[HFe_4(CO)_{12}]$ (yield 0.49 g, 88% based on Fe). The salt is soluble in CH_3CN, *N*,*N*-dimethylformamide (DMF), and dimethyl sulfoxide (DMSO).

Other salts of the same cluster can be obtained by using the same procedure and replacing $[NEt_4]Br$ during precipitation with the appropriate tetraalkylammonium salts, e.g., $[NMe_4]^+$, $[NBu_4]^+$, or $[NMe_3(CH_2Ph)]^+$. With the same procedure, $[HNEt_3][HFe_3(CO)_{11}]$ can be used instead of $[Fe(DMF)_6][Fe_4(CO)_{13}]$ as the starting material.

Elem anal. Calcd for $C_{36}H_{61}Fe_4N_3O_{12}$ (951.28): C, 45.45; H, 6.46; N, 4.42; Fe, 23.48. Found: C, 45.58; H, 6.29; N, 4.22; Fe, 23.57. IR (CH_3CN, 293 K): ν(CO) 1964(w), 1884(vs), 1833(m), 1707(ms) cm^{-1}. ESI-MS (CH_3CN; relative intensity in parentheses): *m*/*z* 280 (100) $[HFe_4(CO)_{12}]^{2-}$; 266 (15) $[HFe_4(CO)_{11}]^{2-}$. ^1H NMR (CD_3CN, 298 K): δ −20.4 ppm. ^{13}C NMR (CD_3CN, 298 K): δ 286 (br), 222 (br) ppm. ^{13}C NMR (CD_3CN, 243 K): δ 286.2 (μ-CO), 227.6 (terminal), 224.1 (terminal), 216.8 (terminal) ppm.

Synthesis of $[NEt_4]_2[HFe_4(CO)_{11}(CO\text{-}Me)]$. CF_3SO_3Me (72 μL, 0.64 mmol) was added dropwise with a micropipette to a solution of $[NEt_4]_3[HFe_4(CO)_{12}]$ (0.59 g, 0.62 mmol) in CH_3CN (20 mL). IR monitoring confirmed the complete conversion of the starting material into the final $[NEt_4]_2[HFe_4(CO)_{11}(CO\text{-}Me)]$ product in ca. 30 min. Thus, the solvent was removed under reduced pressure, and the residue washed with water (20 mL) and THF (20 mL) and finally extracted in acetone (20 mL). Evaporation of the latter gave a microcrystalline powder of $[NEt_4]_2[HFe_4(CO)_{11}(COMe)]$ (yield 0.46 g, 89%).

The salt is soluble in acetone, CH_3CN, DMF, and DMSO and sparingly soluble in THF. The compound is stable in a solid, but in solution, it decomposes within 24 h, yielding $[Fe_4(CO)_{13}]^{2-}$ as the main product. Therefore, all attempts to grow crystals of $[HFe_4(CO)_{11}(CO\text{-}Me)]^{2-}$ suitable for X-ray analysis (independently on the $[NR_4]^+$ cation or the solvent employed) failed, resulting systematically in the isolation of $[Fe_4(CO)_{13}]^{2-}$.

Elem anal. Calcd for $C_{29}H_{44}Fe_4N_2O_{12}$ (836.05): C, 41.66; H, 5.30; N, 3.35; Fe, 26.72. Found: C, 41.85; H, 5.41; N, 3.18; Fe, 26.57. IR (CH_3CN, 293 K): ν(CO) 1935(vs), 1833(m), 1754(ms) cm^{-1}. ^1H NMR (CD_3CN, 298 K): δ −22.9 (1H, μ_3-H), 4.4 (3H, COMe) ppm. ^{13}C NMR (CD_3CN, 243 K): δ 351.1 (μ-*C*OMe), 274.6 (μ-CO), 222.4, 221.9, 219.1, 215.2, 214.7 (terminal CO's), 67.1 (μ-CO*Me*) ppm.

X-ray Crystallographic Study. Crystal data and collection details for $[NEt_4]_3[HFe_4(CO)_{12}]$ are reported in Table 1. The diffraction experiments were carried out on a Bruker APEX II diffractometer equipped with a CCD detector using Mo Kα radiation. Data were corrected for Lorentz polarization and absorption effects (empirical absorption correction with *SADABS*).[17] Structures were solved by direct methods and refined by full-matrix least squares based on all data using F^2.[18] The asymmetric unit contains two independent $[HFe_4(CO)_{12}]^{3-}$ anions and six $[NEt_4]^+$ cations. Hydrogen atoms bonded to carbon atoms were fixed at calculated positions and refined by a riding model. The hydrides bonded to the metal cage in both of the independent anions were located in the Fourier map and refined isotropically with distance restraints similar to those of the Fe_3 triangle (SADI instruction in *SHELX*, s.u. 0.01). The correct location of the hydrides was also confirmed by using the program *XHYDEX*.[19] All non-hydrogen atoms were refined with anisotropic displacement parameters, unless otherwise stated. After location of all of the atoms in $[NEt_4]_3[HFe_4(CO)_{12}]$, some residual electron density remained in the center of the four triangular faces of each Fe_4 tetrahedron. This was interpreted as partial disorder in the cluster anions. Thus, the minor images of the two Fe_4 tetrahedra were included in the final

(13) Whitmire, K. H.; Shriver, D. F. *J. Am. Chem. Soc.* **1981**, *103*, 6754.
(14) (a) Inkrott, K. E.; Shore, S. G. *Inorg. Chem.* **1979**, *18*, 2817. (b) Suter, R.; Bhattacharyya, A. A.; Hsu, L.-Y.; Krause Bauer, J. A.; Shore, S. G. *Polyhedron* **1998**, *17*, 2889. (c) Jackson, P. F.; Johnson, B. F. G.; Lewis, J. *J. Chem. Soc. Chem. Commun.* **1978**, 920. (d) Wilson, R. D.; Wu, S. M.; Love, R. A.; Bau, R. *Inorg. Chem.* **1978**, *17*, 1271.
(15) (a) Johnson, B. F. G.; Lewis, J.; Raithby, P. R.; Sheldrick, G. M.; Suss, G. *J. Organomet. Chem.* **1978**, *162*, 179. (b) McPartlin, M.; Nelson, W. J. H. *J. Chem. Soc., Dalton Trans.* **1986**, 1557. (c) Johnson, B. F. G.; Lewis, J.; Raithby, P. R.; Zuccaro, C. *Acta Crystallogr.* **1981**, *B37*, 1728.
(16) Keller, E. *SCHAKAL99*; University of Freiburg: Freiburg, Germany, 1999.
(17) Sheldrick, G. M. *SADABS, Program for empirical absorption correction*; University of Göttingen: Göttingen, Germany, 1996.
(18) Sheldrick, G. M. *SHELX97, Program for crystal structure determination*; University of Göttingen: Göttingen, Germany, 1997.
(19) Orpen, A. G. *J. Chem. Soc., Dalton Trans.* **1980**, 2509.

Table 1. Crystal Data and Experimental Details for $[NEt_4]_3[HFe_4(CO)_{12}]$

formula	$C_{36}H_{61}Fe_4N_3O_{12}$
fw	951.28
T, K	293(2)
λ, Å	0.710 73
cryst syst	monoclinic
space group	$P2_1/c$
a, Å	23.979(3)
b, Å	16.887(2)
c, Å	23.202(3)
β, deg	113.636(2)
cell volume, Å^3	8607.4(19)
Z	8
D_c, g cm^{-3}	1.468
μ, mm^{-1}	1.381
F(000)	3984
cryst size, mm	0.22 × 0.15 × 0.12
θ limits, deg	1.52−26.00
index ranges	$-29 \le h \le 29$ $-20 \le k \le 20$ $-28 \le l \le 28$
reflns collected	85 181
independent reflns	16 807 [$R_{int} = 0.0644$]
completeness to θ_{max} (%)	99.3
data/restraints/param	16 807/312/1064
GOF on F^2	1.031
R1 [$I > 2\sigma(I)$]	0.0658
wR2 (all data)	0.2059
largest diff peak and hole, e Å^{-3}	+0.822/−0.551

refinement, giving refined occupancy factors of 0.973 62 and 0.981 83 for the main images of each Fe_4 tetrahedron in the two independent anions. Because the minor images represent less than 3% of the whole structure, only their iron atoms have been located and included in the model.

One $[NEt_4]^+$ cation is disordered, and therefore its atomic positions were split and refined isotropically using similar U restraints and one occupancy parameter per disordered group. Similar U restraints were applied also to all carbon and oxygen atoms (s.u. 0.005) and iron atoms (s.u. 0.01). Restraints to bond distances were applied to all of the $[NEt_4]^+$ cations as follows: 1.47 Å (s.u. 0.01) for C−N and 1.53 Å (s.u. 0.01) for C−C.

Results and Discussion

1. Synthesis and Spectroscopic Characterization of $[HFe_4(CO)_{12}]^{3-}$. The $[HFe_4(CO)_{12}]^{3-}$ trianion has been obtained in high yields by stirring under nitrogen $K_2[Fe_4(CO)_{13}]$ in a methylalcoholic solution of KOH (6 M) and precipitation by metathesis with tetrasubstituted ammonium halides. The reaction (1) is straightforward and, according to well-accepted mechanisms,[1a] consists of a nucleophilic attack at a carbon monoxide group to give a $[Fe_4(CO)_{12}(COOH)]^{3-}$ metallacarboxylic acid, which readily eliminates CO_2, while the hydrogen atom migrates to the iron cluster cage. Unfortunately, the absorbance of the methylalcoholic KOH solutions is too high and hinders monitoring by IR of the reaction.

$$[Fe_4(CO)_{13}]^{2-} + 2OH^- \rightarrow [HFe_4(CO)_{12}]^{3-} + HCO_3^- \quad (1)$$

In a less straightforward manner, the same dark-red compound has also been obtained by reacting $[HNEt_3][HFe_3(CO)_{11}]$ in 6 M methylalcoholic KOH solutions with very similar yields, formally following eq 2.

$$4[HFe_3(CO)_{11}]^- + 7OH^- \rightarrow 3[HFe_4(CO)_{12}]^{3-} + 2HCO_3^- + 6CO + 3H_2O \quad (2)$$

Remarkably, the monohydride cluster $[HRu_4(CO)_{12}]^{3-}$ is reported to be unstable in solution toward disproportionation into the corresponding $[H_2Ru_4(CO)_{12}]^{2-}$ and $[Ru_4(CO)_{12}]^{4-}$.[14a] In contrast, the iron congener $[HFe_4(CO)_{12}]^{3-}$ monohydride is stable under a nitrogen atmosphere both in the solid state and in solution (even for several days and independently on the solvent employed) and is, by far, the most stable species of the $[H_{4-n}Fe_4(CO)_{12}]^{n-}$ series (see the next section). It quantitatively disproportionates only under a CO atmosphere according to reaction (3).

$$[HFe_4(CO)_{12}]^{3-} + 3CO \rightarrow [HFe(CO)_4]^- + [Fe_3(CO)_{11}]^{2-} \quad (3)$$

The $[NEt_4]_3[HFe_4(CO)_{12}]$ salt has been characterized by elemental analysis, ESI-MS, IR, and ^{1}H and ^{13}C NMR spectroscopy, and X-ray analysis.

The ESI-MS spectrum displays a main feature at m/z 280 attributable to an oxidized $[HFe_4(CO)_{12}]^{2-}$ ion and a minor peak centered at m/z 266, due to loss of one CO ligand. The IR spectrum displays the presence of terminal and edge-bridging carbonyl ligands, both in solution [ν(CO) in MeCN at 1964(w), 1884(s), 1833(m), and 1707(ms) cm^{-1}] and in Nujol mull. The ^{1}H NMR spectrum in CD_3CN at 298 K shows the presence of a high-field resonance at δ −20.4 ppm. The chemical shift of the unique hydride atom does not vary by changing the temperature or the solvent (i.e., δ −20.4 ppm also in DMSO-d^6). Owing to reaction (3), a ^{13}CO-enriched sample has been prepared by first enriching a sample of $[HFe_3(CO)_{11}]^-$ under a ^{13}CO atmosphere, followed by its conversion into $[HFe_4(CO)_{12}]^{3-}$ according to eq 2. The ^{13}C NMR spectrum of $[HFe_4(CO)_{12}]^{3-}$ (ca. 30% ^{13}CO-enriched) is temperature-dependent because of ligand fluxionality. Thus, as shown in Figure 1a, at 298 K two extremely broad resonances at ca. δ 286 and 222 ppm are observed. The sharp resonances at ca. δ 231, 228.5, and 224 ppm are due to some $[Fe_3(CO)_{11}]^{2-}$, $[Fe_2(CO)_8]^{2-}$, and $[Fe_4(CO)_{13}]^{2-}$, respectively, which are often found as byproducts of reaction (2). The fast-exchange limit could not be obtained because of the thermal decomposition of the sample. Conversely, the slow-exchange limit spectrum is already attainable at 243 K. As shown in Figure 1b, it consists of four equally intense resonances at δ 286.2, 227.6, 224.1, and 216.8 ppm, as was expected from the solid-state structure (see the next section). The low-field signal at δ 286.2 ppm is attributable to three equivalent edge-bridging CO ligands. According to the idealized C_{3v} symmetry of the ion, the nine terminal ligands are divided into three sets, each comprising three equivalent carbon monoxide groups, namely, the three CO's bonded to the apical iron atom, the three basal CO's pointing toward the apical $Fe(CO)_3$ fragment, and the three basal CO's pointing in the opposite direction.

2. Protonation and Methylation of $[HFe_4(CO)_{12}]^{3-}$. IR monitoring of the stepwise protonation of $[HFe_4(CO)_{12}]^{3-}$

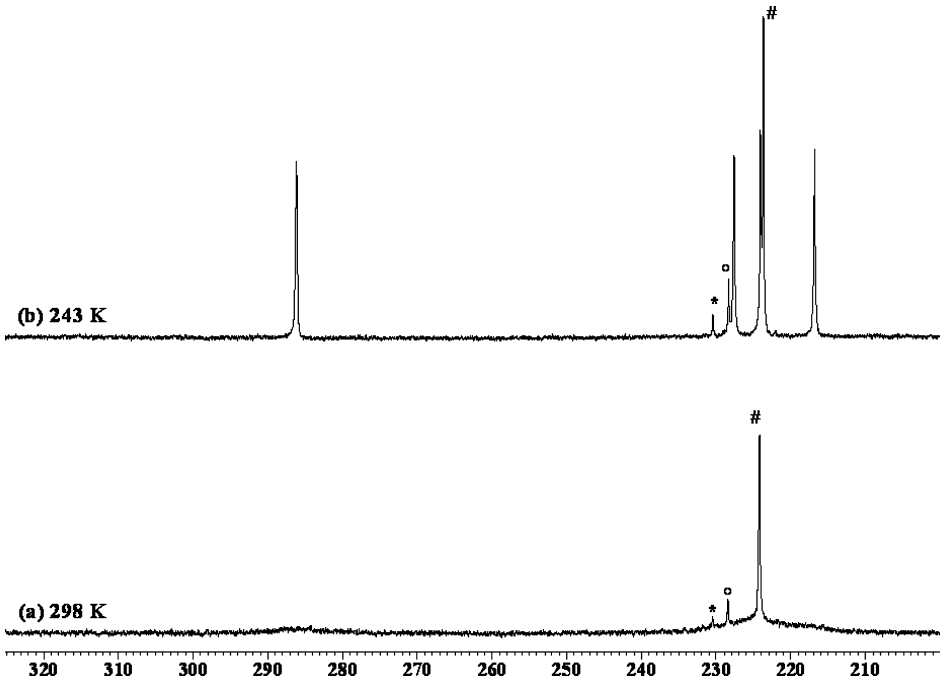

Figure 1. $^{13}C\{^1H\}$ NMR spectra of $[HFe_4(CO)_{12}]^{3-}$ (ca. 30% ^{13}CO-enriched) in CD_3CN at (a) 298 K and (b) 243 K (impurities of $[Fe_4(CO)_{13}]^{2-}$ (#), $[Fe_3(CO)_{11}]^{2-}$ (*), and $[Fe_2(CO)_8]^{2-}$ (○)).

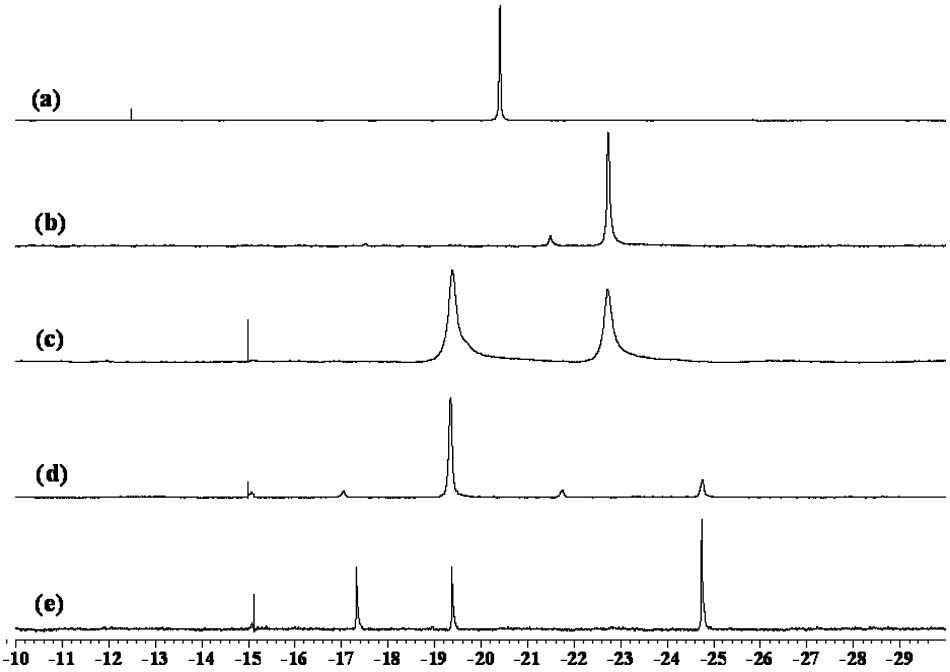

Figure 2. ^1H NMR spectra of $[HFe_4(CO)_{12}]^{3-}$ in CD_3CN at 243 K (a); +1 equiv of HBF_4 immediately after the addition (b); after 10 min (c); after 20 min (d); after an increase in the temperature at room temperature (e).

gives unambiguous evidence for the formation of the $[H_2Fe_4(CO)_{12}]^{2-}$ [ν(CO) at 1935(s) and 1754(m) cm^{-1}] dianion. Unfortunately, this conjugate acid of $[HFe_4(CO)_{12}]^{3-}$ is not sufficiently stable to allow isolation and crystallization. In solution at room temperature, it slowly evolves H_2 and some CO and converts into a complex mixture of products, among which $[Fe_4(CO)_{13}]^{2-}$, $[HFe_4(CO)_{13}]^-$, $[HFe_3(CO)_{11}]^-$, and $[HFe(CO)_4]^-$ have been identified. As soon as obtained, $[H_2Fe_4(CO)_{12}]^{2-}$ is almost quantitatively deprotonated to the parent $[HFe_4(CO)_{12}]^{3-}$ conjugate base by drying its solution under vacuum and dissolving the residue in DMSO.

A more detailed insight on the protonation of $[HFe_4(CO)_{12}]^{3-}$ has been obtained by monitoring the reaction by ^1H NMR in CD_3CN at 243 K (Scheme 1 and Figure 2).

The ^1H NMR spectrum in the hydride region of $[HFe_4(CO)_9(\mu\text{-}CO)_3]^{3-}$ (δ −20.4 ppm) is shown in Figure 2a for the sake of comparison. The addition of $HBF_4 \cdot Et_2O$ at low temperature causes the appearance of a new resonance at −22.7 ppm attributable to the new species $[HFe_4(CO)_9(\mu\text{-}CO)_2(\mu\text{-}CO\text{-}H)]^{2-}$, which progressively increases upon the addition of further $HBF_4 \cdot Et_2O$ and reaches its maximum intensity after the addition of 1 equiv of the acid (Figure 2b). In a

Scheme 1

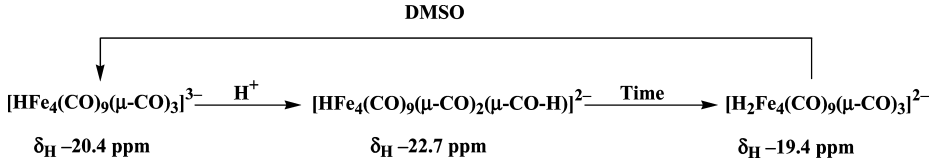

matter of minutes, however, the ^{1}H NMR spectrum evolves as shown in Figure 2c,d, because of the complete conversion of $[HFe_4(CO)_{11}(CO\text{-}H)]^{2-}$ into $[H_2Fe_4(CO)_{12}]^{2-}$, in ca. 20 min at 243 K. This exhibits a unique hydride resonance shifted at low field (δ −19.4 ppm) with respect to the parent $[HFe_4(CO)_{12}]^{3-}$ (δ −20.4 ppm; Figure 2a) and $[HFe_4(CO)_9(\mu\text{-}CO)_2(\mu\text{-}CO\text{-}H]^{2-}$ (δ −22.7 ppm; Figure 2b) compounds. The ^{1}H NMR spectrum further evolves after an increase in the temperature to room temperature. Thus, as shown in Figure 2e, the resonance at δ −19.4 ppm due to $[H_2Fe_4(CO)_{12}]^{2-}$ progressively decreases and new hydride resonances matching those of $[HFe_3(CO)_{11}]^-$ and the two isomers of $[HFe_4(CO)_{13}]^{-}$[20] (in order toward upfield) appear and rapidly become the prevailing species. A yet unknown impurity giving rise to the weak signal at ca. δ −21.8 ppm is sometimes present.

Attempts to further corroborate the above assignments by ^{13}C NMR had little success because of the limited stability of both isomeric $[HFe_4(CO)_9(\mu\text{-}CO)_2(\mu\text{-}CO\text{-}H]^{2-}$ and $[H_2Fe_4(CO)_{12}]^{2-}$ conjugated acids and the complexity of the resulting mixtures.

The assignment of the resonance at δ −22.7 ppm to the dianion $[HFe_4(CO)_9(\mu\text{-}CO)_2(\mu\text{-}CO\text{-}H)]^{2-}$ is supported by the fact that a similar high-field shift of the hydride resonances of $[HFe_3(CO)_{11}]^-$ and $[HFe_4(CO)_{13}]^-$ of ca. 2 ppm was observed by Shriver et al. upon protonation in CD_2Cl_2 at 183 K in an attempt to obtain the purported $[H_2Fe_3(CO)_{11}]$ and $[H_2Fe_4(CO)_{13}]$ dihydrides. Conversely, it has been demonstrated that the upfield shift was due to the formation of the $[HFe_3(CO)_{10}(CO\text{-}H)]$ and $[HFe_4(CO)_{12}(CO\text{-}H]$ adducts by detection of equally intense low-field resonances (δ 15 and 13.2 ppm, respectively) attributable to the oxygen-bound protons and by comparison of their ^{1}H and ^{13}C NMR spectra with those of methylated homologues.[12,13] In our case, a distinct resonance for the oxygen-bound proton could not be observed, probably because of fast exchange with the solvent or moisture and because temperatures lower than 243 K were precluded by the acetonitrile solvent employed and the poor solubility of all $[NR_4]_3[HFe_4(CO)_{12}]$ salts in most other organic solvents. To further implement this suggestion, we investigated, therefore, the methylation of $[HFe_4(CO)_9(\mu\text{-}CO)_3]^{3-}$ with CF_3SO_3Me in acetonitrile.

IR monitoring shows that the progressive addition of 1 equiv of CF_3SO_3Me gives rise to the quantitative formation of the corresponding $[HFe_4(CO)_9(\mu\text{-}CO)_2(\mu\text{-}CO\text{-}Me)]^{2-}$ derivative, which is fairly stable at room temperature in solution, at least to allow complete spectroscopic characterization. It shows IR carbonyl absorptions at 1934(s) and 1749(m) cm^{-1} and ^{1}H NMR resonances at δ −22.9 and 4.4 (μ-CO-Me) ppm in a 1:3 ratio. The ^{13}C NMR spectrum shows seven signals of relative intensities 1:2:2:2:1:1:3:1 at 351.1 (1; μ-*C*OMe), 274.6 (2; μ-CO), 222.4 (2), 221.9 (2), 219.1 (1), 215.2 (1), 214.7 (3), and 67.1 (1; μ-CO*Me*) ppm. Such a pattern is in keeping with the reduced C_s symmetry expected for a $[HFe_4(CO)_9(\mu\text{-}CO)_2(\mu\text{-}CO\text{-}Me)]^{2-}$ adduct. Moreover, its hydride resonance at δ_H −22.9 ppm is very similar to the δ_H value (−22.7 ppm) assigned to the hydride resonance of the related $[HFe_4(CO)_9(\mu\text{-}CO)_2(\mu\text{-}CO\text{-}H)]^{2-}$ dianion and further corroborates the protonation reaction reported in Scheme 1.

Unfortunately, all attempts to grow crystals suitable for the X-ray analysis of $[HFe_4(CO)_9(\mu\text{-}CO)_2(\mu\text{-}CO\text{-}Me)]^{2-}$ have failed, resulting systematically in the isolation of $[Fe_4(CO)_{13}]^{2-}$. Thus, it seems likely that the $[HFe_4(CO)_9(\mu\text{-}CO)_2(\mu\text{-}CO\text{-}Me)]^{2-}$ dianion is not stable enough in solution for allowing crystallization. This is well corroborated by IR and ESI-MS analyses on the $[HFe_4(CO)_{11}(\mu\text{-}CO\text{-}Me)]^{2-}$ solutions, which clearly indicate complete decomposition within 24 h, yielding $[Fe_4(CO)_{13}]^{2-}$ as the main product.

Finally, the presence of edge-bridging carbonyls in the IR spectrum of $[H_2Fe_4(CO)_9(\mu\text{-}CO)_3]^{2-}$, the equivalence of its two hydride atoms, as indicated by ^{1}H NMR, and their chemical shift, which is very similar to that of the fully characterized $[H_2Ru_4(CO)_9(\mu\text{-}CO)_3]^{2-}$ congener,[14a] suggest that the two are isostructural.

3. X-ray Structure of $[HFe_4(CO)_9(\mu\text{-}CO)_3]^{3-}$. The $[NEt_4]_3[HFe_4(CO)_{12}]$ salt has been characterized by X-ray diffraction analysis. The asymmetric unit of $[NEt_4]_3[HFe_4(CO)_{12}]$ contains six $[NEt_4]^+$ cations and two $[HFe_4(CO)_{12}]^{3-}$ anions, which display the same connectivity and only minor differences in their bonding parameters. The structure of the trianion is shown in Figure 3, and the most

Molecular structure of $[HFe_4(CO)_{12}]^{3-}$

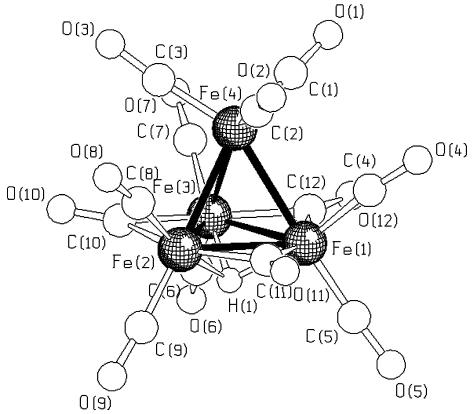

Figure 3. Molecular structure of $[HFe_4(CO)_{12}]^{3-}$.

(20) Horwitz, C. P.; Shriver, D. F. *Organometallics* **1984**, *3*, 756.

Table 2. Main Bonding Distances in $[HFe_4(CO)_{12}]^{3-}$

	molecule 1	molecule 2
Fe(1)−Fe(2)	2.5370(12)	2.5301(12)
Fe(1)−Fe(3)	2.5218(12)	2.5286(12)
Fe(2)−Fe(3)	2.5380(12)	2.5447(12)
Fe(1)−Fe(4)	2.6337(12)	2.6287(12)
Fe(2)−Fe(4)	2.6308(13)	2.6328(12)
Fe(3)−Fe(4)	2.6186(13)	2.6201(12)
Fe(1)−H(1)	1.71(3)	1.75(4)
Fe(2)−H(1)	1.71(3)	1.75(4)
Fe(3)−H(3)	1.71(3)	1.75(4)

relevant bonding distances for the two independent molecular ions are collected in Table 2.

The whole cluster anion and the metal core possess an idealized C_{3v} symmetry based on an elongated Fe_4 tetrahedron. The apical iron atom [Fe(4)] is bonded to three terminal CO ligands, whereas the three basal iron atoms [Fe(1), Fe(2), and Fe(3)] are bonded to two terminal (one below and one above the basal plane) and two edge-bridging carbonyls. The unique hydride ligand is μ_3-coordinated to the Fe_3 basal face. Its location was indicated by residual electron density in the final Fourier difference maps and further supported by a minimum in the nonbonded potential energy surface of the cluster by the program *XHYDEX*.[19] The hydride atom has been included in the final refinements of the structure. The average Fe−H contacts are respectively 1.71(3) and 1.75(4) Å for the two independent molecules. These Fe−H bonding distances can be compared with the value of 1.79(7) Å for the μ-coordinated hydride in $[HFe_3(CO)_{11}]^-$.[8b] The Fe−Fe interactions within the basal plane [range 2.5218(12)−2.5380(12) Å; average 2.53 Å] are significantly shorter than the ones between the apical Fe(4) and the basal triangle [range 2.6186(13)−2.6337(12) Å; average 2.63 Å], with all being spanned by CO bridges.

Several tetrahedral clusters containing 12 CO ligands and one hydride are known. Of these, three species, namely, $[HFe_3Rh(CO)_{12}]^{2-}$,[21] $[HFe_3Ir(CO)_{12}]^{2-}$,[22] and $HCo_3Ru(CO)_{12}$,[23] display exactly the same stereochemistry of $[HFe_4(CO)_{12}]^{3-}$. Conversely, $[HFe_3Ni(CO)_{12}]^-$[24] and $[HRu_3Ni(CO)_{12}]^-$[25] possess a related coordination sphere only differing in the bending of one terminal CO of the basal nickel atom toward the apical iron or ruthenium atom, which gives rise to a fourth μ-CO ligand. Finally, $[HRu_2Rh_2(CO)_{12}]^-$[26] displays the same CO stereochemistry of $[HFe_4(CO)_{12}]^{3-}$ but differs in the stereochemistry of the unique hydride atom, which spans an edge between the apex and the base of the cluster.

The location of the hydride ligand on the basal face of $[HFe_4(CO)_{12}]^{3-}$ is nicely in keeping with the results of extended Hückel molecular orbital (EHMO) calculations with CACAO,[27] which assigns the nature of a Lewis base to a purported $[Fe_4(CO)_{12}]^{4-}$ tetraanion. As shown in Figure 4a, the highest occupied molecular orbital (HOMO) of $[Fe_4(CO)_{12}]^{4-}$ is an in-phase combination of s, p, and d atomic orbitals directed toward the center of the basal Fe_3 face and contains a lone pair. Its combination with the s atomic orbital of H^+ generates an in-phase MO (Figure 4b), which sinks in the bonding region, and a high-lying out-of-phase MO. The resulting $[HFe_4(CO)_{12}]^{3-}$ compound displays a wide HOMO−LUMO gap of ca. 2.1 eV (Figure 4c), in agreement with its electron-precise (60 cluster valence electrons) closed-shell configuration. Such a result is in keeping with its lack of reversible redox behavior.

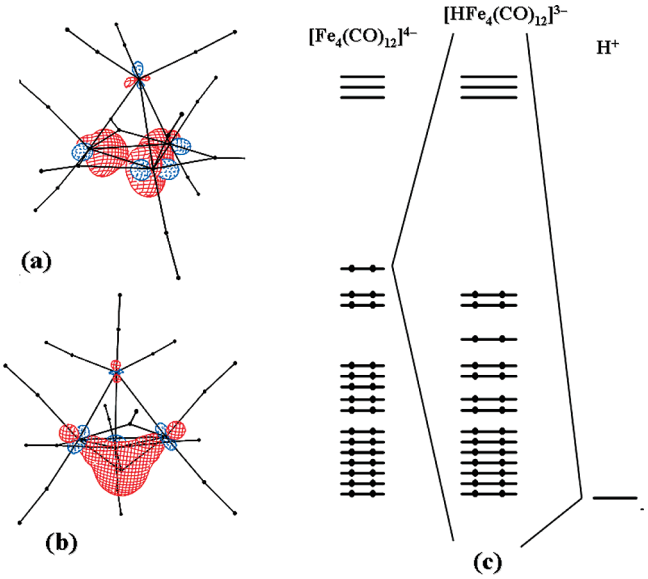

Figure 4. (a) HOMO of $[Fe_4(CO)_{12}]^{4-}$. (b) Bonding MO resulting from the combination of that in part a and H^+. (c) Frontier region (in the −13.6 to −9 eV energy interval) of the EHMO diagram of $[HFe_4(CO)_{12}]^{3-}$.

Conclusions

In summary, a new iron carbonyl anion, i.e., $[HFe_4(CO)_{12}]^{3-}$, has been obtained in high yields by a straightforward synthesis and fully characterized. Spectroscopic proof for the existence of its unstable isomeric $[HFe_4(CO)_{11}(CO\text{-}H)]^{2-}$ and $[H_2Fe_4(CO)_{12}]^{2-}$ conjugated acids has also been obtained. The latter is probably isostructural with the $[H_2Ru_4(CO)_{12}]^{2-}$ congener. The nature of the first protonation product as a $[HFe_4(CO)_{11}(CO\text{-}H)]^{2-}$ adduct, involving an oxygen-bound proton, has been implemented by isolation and characterization of the corresponding $[HFe_4(CO)_{11}(CO\text{-}Me)]^{2-}$ dianion. First of all, the above findings demonstrate that protonation of a CO-shielded polynuclear metal anion initially occurs on one oxygen atom and then the oxygen-bound proton migrates to the iron atoms to form Fe−H bonds. This result relates and provides insight into the mechanism of hydrogen transfer in related reactions, such as the formation of $[HRu_3(CO)_{11}]^-$ from $Ru_3(CO)_{12}$.[28]

Second, $[HFe_4(CO)_{12}]^{3-}$ and its $[H_2Fe_4(CO)_{12}]^{2-}$ conjugate acid fill the previously existing gap between the chemistry of iron carbonyls and ruthenium and osmium congeners.

(21) Della Pergola, R.; Garlaschelli, L.; Demartin, F.; Manassero, M.; Masciocchi, N.; Longoni, G. *J. Organomet. Chem.* **1988**, *352*, C59.
(22) Ceriotti, A.; Della Pergola, R.; Garlaschelli, L.; Laschi, F.; Manassero, M.; Masciocchi, N.; Sansoni, M.; Zanello, P. *Inorg. Chem.* **1991**, *30*, 3349.
(23) Pursiainen, J.; Hirva, P.; Pakkanen, T. A. *J. Organomet. Chem.* **1991**, *419*, 193.
(24) Ceriotti, A.; Chini, P.; Fumagalli, A.; Koetzle, T. F.; Longoni, G.; Takusagawa, F. *Inorg. Chem.* **1984**, *23*, 1363.
(25) Brivio, E.; Ceriotti, A.; Della Pergola, R.; Garlaschelli, L.; Manassero, M.; Sansoni, M. *J. Cluster Sci.* **1995**, *6*, 271.
(26) Fumagalli, A.; Italia, D.; Malatesta, M. C.; Ciani, G.; Moret, M.; Sironi, A. *Inorg. Chem.* **1996**, *35*, 1765.
(27) Mealli, C.; Proserpio, D. M. *J. Chem. Educ.* **1990**, *66*, 399.

Such a late report regarding the isolation and characterization of a new series of hydridocarbonylferrates may appear surprising because iron carbonyls have been extensively studied for more than a century. However, it has to be taken into account that earlier recognition of the existence of $[HFe_4(CO)_{12}]^{3-}$, as well as its $[H_2Fe_4(CO)_{12}]^{2-}$ conjugate acid, has probably been hampered and hindered by the similarity of their IR absorptions with those of $[HFe(CO)_4]^-$ and mixtures of $[Fe_3(CO)_{11}]^{2-}$ and $[Fe_4(CO)_{13}]^{2-}$.

The ready availability of stable $[HFe_4(CO)_{12}]^{3-}$ salts now provides a new tetranuclear iron carbonyl anion exhibiting the lowest CO/Fe ratio and a relatively high negative charge per iron atom, which might represent a possible starting material for the preparation of new species.

(28) (a) Bricker, J. C.; Nagel, C. C.; Shore, S. G. *J. Am. Chem. Soc.* **1982**, *104*, 1444. (b) Bricker, J. C.; Nagel, C. C.; Bhattacharyya, A. A.; Shore, S. G. *J. Am. Chem. Soc.* **1985**, *107*, 377.

Acknowledgment. We acknowledge funding from the University of Bologna (CLUSTERCAT) and MIUR (PRIN2006).

Supporting Information Available: Crystallographic data in CIF format for $[NEt_4]_3[HFe_4(CO)_{12}]$. This material is available free of charge via the Internet at http://pubs.acs.org.

IC802015F